Int. J. Electrochem. Sci., 9 **(2014)** 1565 - 1582

International Journal of
ELECTROCHEMICAL
SCIENCE
www.electrochemsci.org

Novel Plant Extracts as Green Corrosion Inhibitors for 7075-T6 Aluminium Alloy in an Aqueous Medium

Howida A. Fetouh[1], *Tarek M. Abdel-Fattah*[2], *Mohamed S. El-Tantawy*[1,*]

[1] Chemistry Department, Faculty of Science, Alexandria University, Ibrahimia, P.O. Box 426, Alexandria 21321, Egypt.
[2] Applied Research Center Thomas Jefferson National Accelerator Facility and Department of Molecular Biology and Chemistry, Christopher Newport University, Newport News, Virginia 23606, USA.
[*]E-mail: mohamed.tantawy1@gmail.com

Received: 7 October 2013 / *Accepted:* 21 December 2013 / *Published:* 5 January 2014

The effect of aqueous extracts of Damsissa, Lupine and Halfa-bar on the corrosion of 7075-T6 aluminium alloy in an aqueous solution of 0.5M sodium chloride has been studied employing electrochemical impedance spectroscopy and potentiodynamic polarization techniques. The impedance (Nyquist) plots manifested that the dissolution process is controlled by charge transfer from anodic to cathodic sites. The polarization curves showed that the three extracts act as cathodic inhibitors. Inhibitive mechanism was discussed assuming the adsorption of the three extracts on the electrode surface. Theoretical fitting of Langmuir, Flory-Huggins adsorption isotherms and the kinetic-thermodynamic model were tested to clarify the adsorption mechanism.

Keywords: Alloys; Electrochemical techniques; Adsorption; Corrosion

1. INTRODUCTION

Aluminium and its alloys have found widespread applications because of their physicochemical and metallurgical characteristics [1] The wrought aluminium-zinc-magnesium copper (AA7000) series alloys are commonly used in the aerospace industry and super-jet boats industry due to their high strength-to-weight ratio, toughness and resistance to fatigue [2, 3] The microstructure of these alloys is heterogeneous and consists of an Al matrix, intermetallic particles (IMPs) and hardening precipitates within the grains, precipitate free zones (PFZ) near the grain boundaries and grain boundary precipitates [4]. Most of the Cu in these alloys is contained in the nanometer size GP (Guinier Preston) zones and ή phase. Cu is also present in the micrometer size IMPs including Al_2CuMg (S phase), Al_2Cu (θ phase) and Al_7CuFe and the grain boundary precipitate $Mg(ZnCuAl)_2$ (η phase). The high

passivity normally associated with aluminium comes from the highly adherent barrier oxide of Al_2O_3 that forms on the surface. In aqueous environments this protective oxide is formed with a greater thickness and, as long as there is oxygen present, it will continue to repassivate if flaws are formed [5]. However, in the presence of chloride ions (Cl^-), such as in sea water, the oxide is broken down [6] and its repair is hindered. Pitting corrosion in 7000 series alloys has been found to occur near Cu and Fe containing intermetallic particles. Both Cu and Fe are more cathodic than the Al matrix resulting in a galvanic interaction. Meng and Frenkel have studied the corrosion behaviour of a series of 7000 alloys with increasing Cu content all in T_6 temper in aerated NaCl, they found that the polarization resistance and the corrosion potential decreased with increasing Cu content. In addition, two breakdown potentials were observed during the potentiodynamic polarization studies. The lower breakdown potential (E_1) was due to transient dissolution associated with the attack of the hardening particles (ή phase), while the second nobler breakdown potential (E_2) was due to stable dissolution at the grain boundaries and selective attack within the grains. Meng and Frenkel showed that in a deaerated NaCl solution, these potentials increased with increasing Cu content. It was concluded that Cu content in the matrix (including the hardening precipitates) controlled this potential [4].

Over the years, the use of chemical inhibitors has been limited because of their environmental threat, and more; recently, because of environmental regulations, Plant extracts are environmentally acceptable and readily available, in addition to being a renewable source for a wide range of corrosion inhibitors. Plant extracts are an incredibly rich source of naturally synthesized chemical compounds that can be extracted by simple procedures with low cost. However, synergistic (and antagonistic) effects are often expected with these mixtures of inhibitors, which may affect their efficiency. For instance, damsissa (*Ambrosia maritima*, L.) is a wild plant present in Egypt and in different African countries in the Nile valley. It contains important sesquiterpene lactones and flavonoids; the most active compounds of this plant are ambrosin and damsin which belongs to a group of natural products known as pseudoguainolides [7]. Seeds of lupine (*Lupinus sp.* L.) contain up to 50% protein, 20% lipids and 5% quinolizidine alkaloids. Analysis of the alkaloid content clarify that the quinolizidine lupine alkaloids especially lupanine were the most abundant; multiflorine was also present. Moreover, lupine extract contains sparteine that is a dibasic quinolizidine alkaloid [8].

Halfa-bar (*Cymbopogon Proximus*) is mainly used in folk medicine. The main chemical compounds found in *Halfa-Bar* are six sesquiterpenes which are: proximadiol (1), 5α-hydroxy-β-eudesmol(2), 5α-hydroperoxy-β-eudesmol(3),1β-hydroxy-β-eudesmol(4),1β-hydroxy-α-eudesmol (5) and 7α, 11-dihydroxy-cadin-10(14)-ene.(6) [9]. The aim of the present work is to investigate the inhibition efficiency of damsissa, lupine and halfa-bar extracts for the corrosion of 7075-T6 aluminium alloy in an aqueous media (seawater and 0.5M NaCl solution) using electrochemical techniques.

2. EXPERIMENTAL

2.1. DC and AC Measurements

Potentiodynamic measurements and impedance measurements have been achieved by connecting the electrochemical cell to a Gill ACM instrument. Because of the presence of a degree of

non-linearity in the anodic polarization curves, cathodic Tafel slope (β_c) was obtained by applying Tafel extrapolation method on the linear part of the cathodic polarization curves by using the computer version 5 software analysis program. The sweep rate was 20mV/min. In the impedance measurements, 10 points were measured for each decade of frequency that ranged between 10 kHz and 0.1 Hz. The amplitude of the superimposed AC potential was 10 mV. All measurements were recorded at the rest potential using three-electrode cell. A saturated calomel electrode, SCE, was used as reference electrode and a platinum sheet sealed in a ground joint as a counter electrode. The material used for constructing the working electrode was pure aluminium with the following chemical composition (wt. %): Zn, 5.50; Mg, 2.60; Cu, 1.98; Fe, 0.48; Si, 0.40; Cr, 0.18; Mn, 0.14; balance Al. An Al-alloy 7075-T6 sheet of 0.2 cm thick was cut into 1.5 cm by 3.0 cm panels, exposing a fixed area of 7.1cm^2 to the test solution. The remaining area was isolated by epoxy and fixed to a Cu wire for electrical connection. The samples were wet hand-polished using different grade emery papers 320, 400, 600 and 1000 grit finishes starting with a coarse one and proceeding in steps to the fine grit up to a mirror finish, washed thoroughly with double-distilled water and finally dried by absolute ethanol just before immersion in the tested solution. Each experiment was carried out with newly polished electrode surface. Duplicate experiments were performed and the good reproducibility of the results was obtained with an experimental error ±2.0.

2.2. Solutions preparation

The solutions were prepared using double distilled water and A.R. chemicals. A stock solution of plant extracts was obtained by refluxing 100.0 g of the dry materials in 500 mL distilled water for 2.0 h. The refluxed solution was filtered to remove any contamination. The concentration of the stock solution was calculated in g.

3. RESULTS AND DISCUSSION

3.1. Potentiodynamic polarization measurements:

Figures (1-3) show the anodic and cathodic polarization curves for 7075-T6 aluminum alloy in 0.5M NaCl at 30^{o}C in absence and presence of different concentrations of Damsissa, Lupine and Halfa bar extracts.

The anodic polarization curves indicate that the active dissolution of the alloy in all tested solutions occur under activation control of the slowest (rate determining) step in the anodic reaction. No pitting corrosion was observed at the high anodic overpotential. The cathodic polarization curves indicate that oxygen gas reduced according to equation (1), which accumulates within the pores of the alloy surface, raising the local pH. The formation of $Al(OH)_3$ gel within the aluminium surface is the limiting factor for the current, as it ties up a considerable quantity of water up to 7.5 mL/ g of aluminium [10].

$$\tfrac{1}{2}\, O_{2\,(g)} + H_2O + 2\, e^- \rightleftharpoons 2\, OH^- \quad \text{(charge transfer step)} \qquad (1)$$

Loss of the protective oxide film on an aluminium surface tends to enhance water reduction reaction producing hydrogen gas [11].

$$Al + 3H_2O \rightleftharpoons Al\,(OH)_3 + 3H^+ + 3e^- \rightleftharpoons Al\,(OH)_3 + 3/2\, H_{2\,(g)} \qquad (2)$$

This reaction lowers the pH value near the aluminium surface which, tends to form a passive film of hydrargillite, $Al_2O_3.3H_2O$ that decreases the corrosion rate and inhibits the anodic dissolution of aluminium. Weak passivity is observed at a relatively high anodic potential at current density ≈ 0.2 mA/cm^2 and potential ($E_{passive}$≈ -700 mV). Chloride ion breaks down the passive layer, causing current density to increase again [8].

As soon as the cathodic sites become completely covered by the reduction products, the current density reaches the limiting value (i_L). By increasing the concentration of plant extracts, the limiting current density decreases. This behavior indicated that all the plant extracts decrease the corrosion rate of the alloy in 0.5M NaCl by retarding the reduction reaction of oxygen gas and water [12]. The plant extracts showed no effect on the anodic oxidation reaction of aluminium but they did shift the cathodic polarization curves to highly negative overpotential. This means that the plant extracts are classified as cathodic type inhibitors.

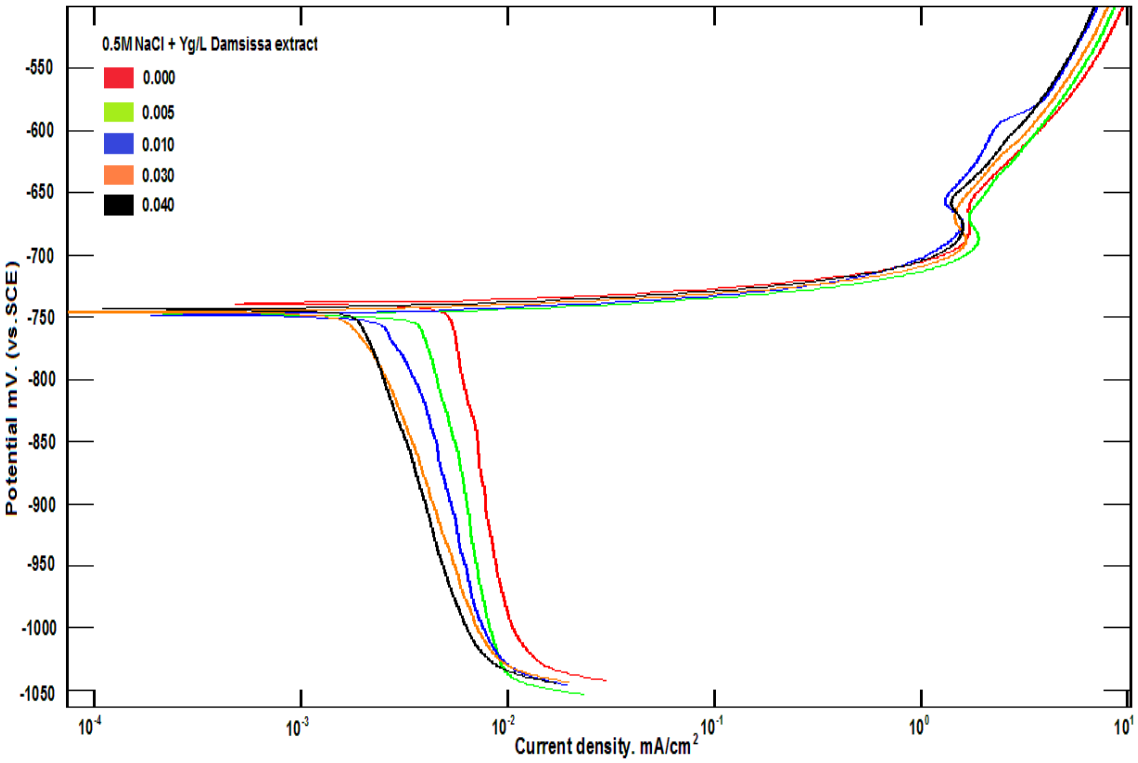

Figure 1. Potentiodynamic polarization curves for 7075-T6 aluminium alloy in0.5M NaCl at 30^{o}C in absence and presence of different concentrations of *Damsissa* extract.

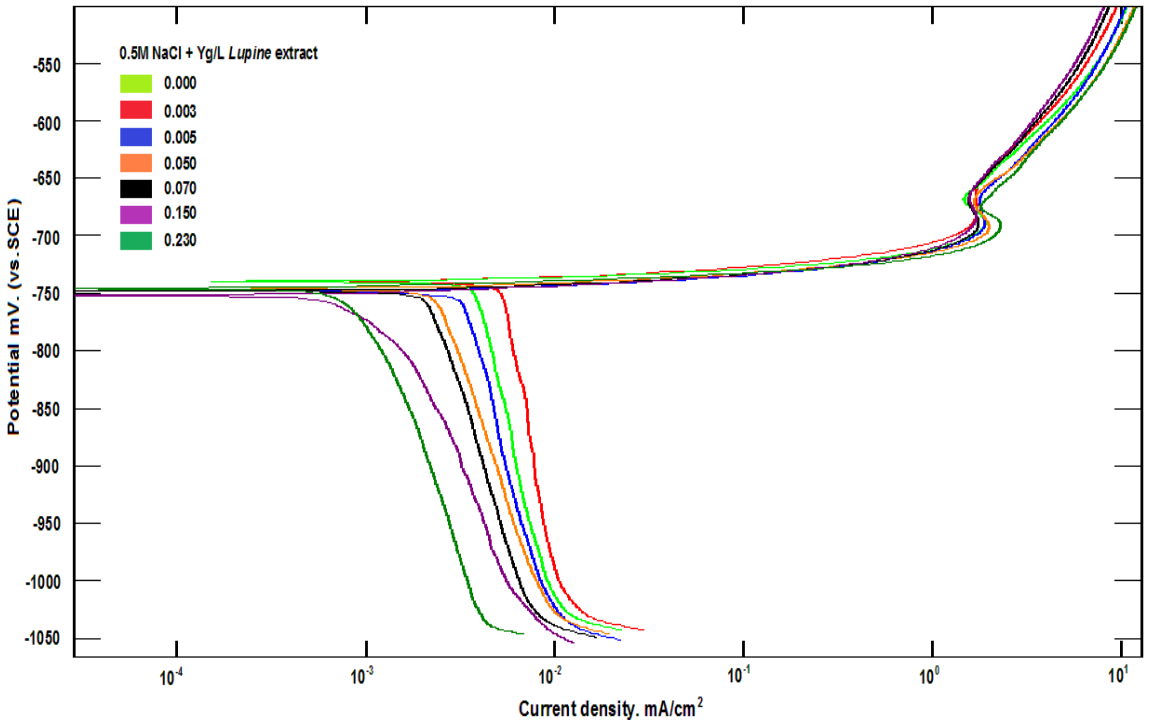

Figure 2. Potentiodynamic polarization curves for 7075-T6 aluminium alloy in 0.5M NaCl at 30°C in absence and presence of different concentration of *Lupine* extract.

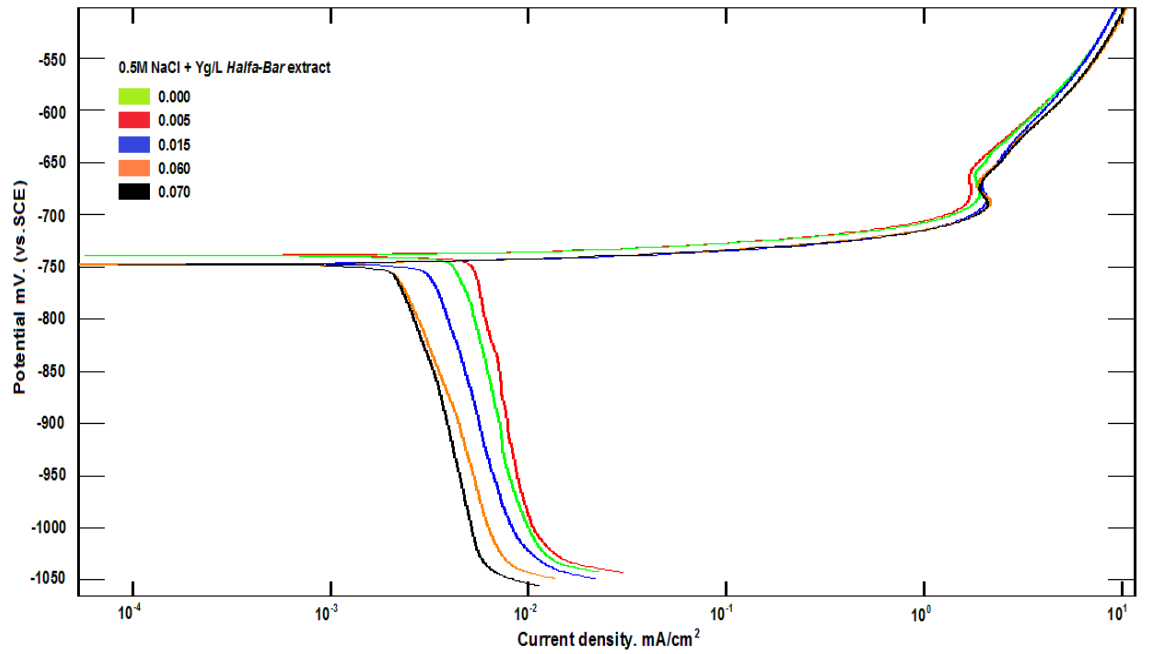

Figure 3. Potentiodynamic polarization curves for 7075-T6 aluminium alloy in 0.5M NaCl at 30^{o}C in absence and presence of different concentration of *Halfa-bar* extract.

The electrochemical parameters for the corrosion of 7075-T6 aluminium alloy in 0.5M NaCl at 30^{o}C in absence and presence of different concentrations of plant extracts are obtained by applying the

Tafel extrapolation method on the linear part of the cathodic polarization curves. Tables (1-3) contain the electrochemical parameters, E_{corr}, i_{corr} and β_c for aluminium alloy in 0.5M NaCl solution in absence and presence of different concentrations of aqueous plant extracts with the percentage of inhibition efficiency (%P) calculated from the following relation:

$$\% P = (i_o - i)/i_o) \times 100$$

Where, i_o and i are the corrosion current density in absence and presence of different concentrations of plant extracts.

Table 1. The potentiodynamic polarization parameters for the corrosion of 7075-T6 aluminium alloy in 0.5M NaCl in absence and presence of different concentrations of Damsissa.

Extract Concentration (g/L)	E_{corr} (mV vs. SCE)	β_c (mV.decade^{-1})	I_{corr} (mA.cm^{-2})	% P
Blank	-736.8	982.2	5.60×10^{-3}	0
0.006	-737.7	831.3	3.90×10^{-3}	30.4
0.008	-745.3	831.3	3.80×10^{-3}	32.1
0.014	-747.1	831.3	3.10×10^{-3}	44.6
0.030	-741.4	831.3	2.26×10^{-3}	59.6
0.040	-741.4	525.5	2.10×10^{-3}	62.5
0.080	-740.4	525.5	2.31×10^{-3}	58.8
0.100	-740.4	501.9	2.50×10^{-3}	55.4

Table 2. The potentiodynamic polarization parameters for the corrosion of 7075-T6 aluminium alloy in 0.5M NaCl in absence and presence of different concentrations of Lupine extract.

Extract Concentration (g/L)	E_{corr} (mV vs. SCE)	β_c (mV.decade^{-1})	I_{corr} (mA.cm^{-2})	% P
Blank	-736.8	982.2	5.60×10^{-3}	0
0.0005	-739.6	812.0	5.30×10^{-3}	5.4
0.0026	-737.0	682.3	4.10×10^{-3}	26.8
0.0035	-738.3	682.3	3.70×10^{-3}	33.9
0.005	-745.6	682.3	3.20×10^{-3}	42.9
0.030	-735.3	518.6	2.90×10^{-3}	48.2
0.050	-744.0	495.7	2.80×10^{-3}	50.0
0.070	-744.7	495.7	2.20×10^{-3}	60.7
0.090	-742.9	434.8	2.10×10^{-3}	62.5
0.150	-748.7	434.8	1.50×10^{-3}	73.2
0.200	-743.2	348.6	1.30×10^{-3}	76.9
0.230	-748.2	454.2	1.00×10^{-3}	82.1
0.260	-741.8	456.9	1.70×10^{-3}	69.6
0.300	-742.4	616.1	2.00×10^{-3}	64.3

Table 3. The potentiodynamic polarization parameters for the corrosion of 7075-T6 aluminium alloy in 0.5M NaCl in absence and presence of different concentrations of *Halfa-Bar* extract.

Extract Concentration (g/L)	E_{corr} (mV vs. SCE)	β_c (mV.decade^{-1})	I_{corr} (mA.cm^{-2})	% P
Blank	-736.8	982.2	5.60 x 10^{-3}	0
0.001	-740.4	616.1	4.70 x 10^{-3}	16.1
0.005	-738.0	825.5	4.60 x 10^{-3}	17.9
0.024	-735.4	825.5	3.9 x 10^{-3}	30.4
0.040	-735.4	692.2	3.1 x 10^{-3}	44.6
0.048	-741.9	454.4	2.80 x 10^{-3}	50.0
0.063	-744.6	454.4	2.30 x 10^{-3}	58.9
0.070	-744.6	753.9	2.18 x 10^{-3}	61.1
0.090	-743.2	523.9	2.40 x 10^{-3}	57.1
0.120	-743.5	523.9	2.80 x 10^{-3}	50.0
0.250	-739.4	523.9	3.10 x 10^{-3}	44.6

The corrosion current density (i_{corr}) decreases with increasing the concentration of each plant extract, so these extracts reduce the corrosion rate of 7075-T6 aluminium alloy in aqueous solution of 0.5M NaCl. The values E_{corr} (vs. SCE) for Damsissa, Lupine and Halfa-Bar were unchanged on increasing the concentration of plants extracts. The high values of cathodic Tafel slopes (β_c) indicate that the cathodic reduction reactions occurs through the oxide film on the alloy surface and the kinetic of the corrosion reaction is controlled by the ohmic drop due to the bubbles of $H_{2(g)}$ on the electrode surface [13,14].

3.2. Impedance measurements:

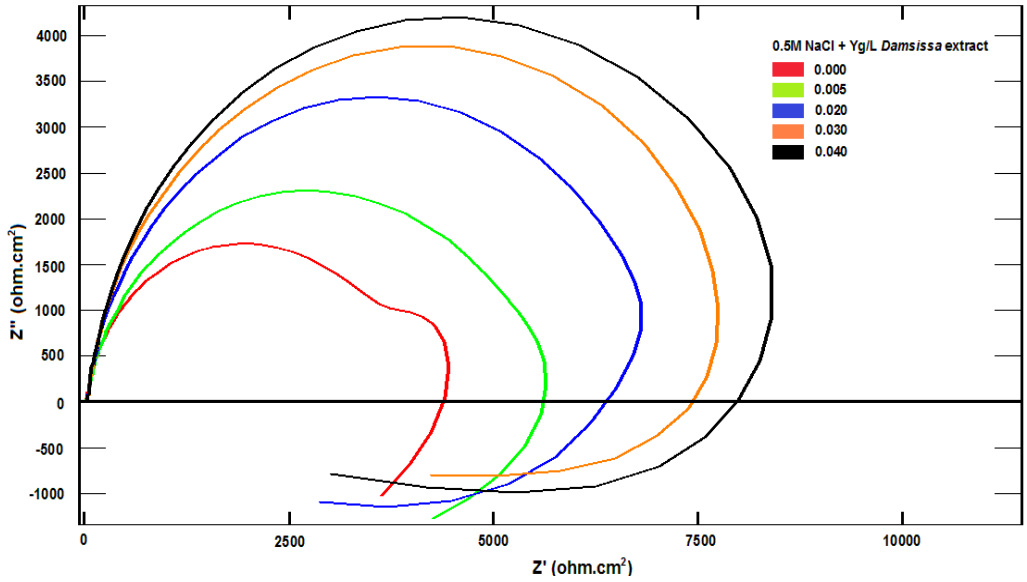

Figure 4. Nyqusit diagrams for corrosion of 7075-T6 aluminium alloy in 0.5M NaCl at30^{o}C in absence and presence of different concentrations of Damsissa extract.

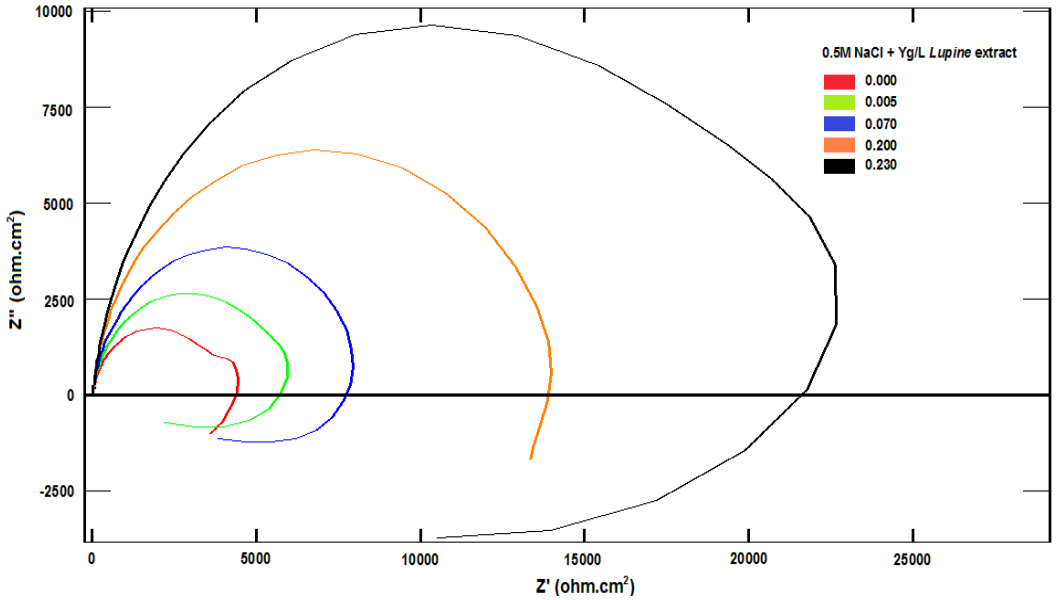

Figure 5. Nyqusit diagrams for corrosion of 7075-T6 aluminium alloy in 0.5M NaCl at 30°C in absence and presence of different concentrations of Lupine extract.

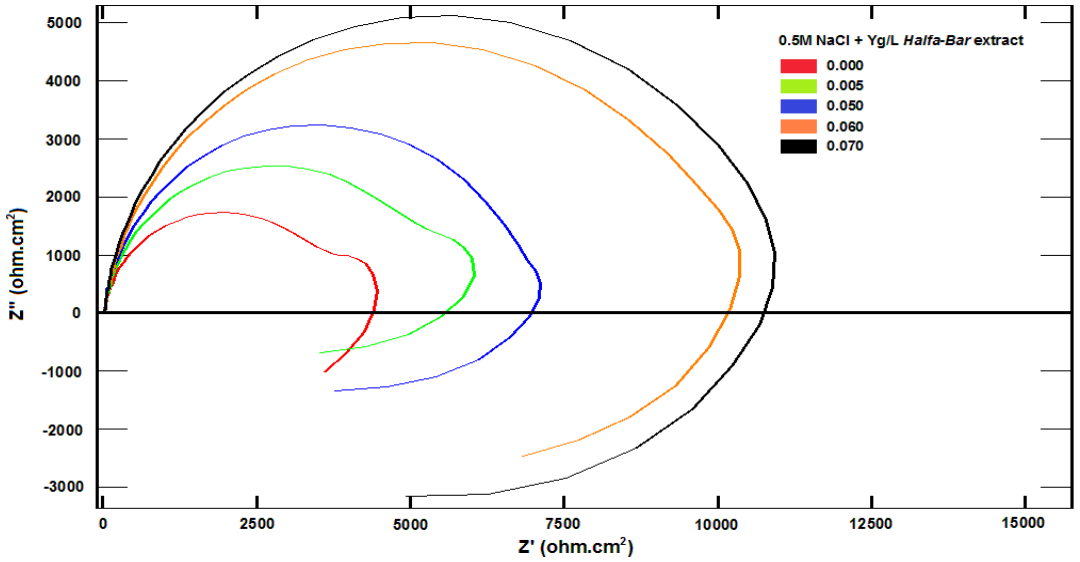

Figure 6. Nyqusit diagrams for corrosion of 7075-T6 aluminium alloy in 0.5M NaCl at30°C in absence and presence of different concentrations of Halfa-Bar extract.

Figures (4-6) represent Nyquist diagrams obtained for 7075-T6 aluminium alloy in 0.5M NaCl at 30°C in absence and presence of different concentrations of Damsissa, Lupine and Halfa-bar extracts.

All of these diagrams have the same appearance of a semicircle with a capacitive loop above the real axis and an inductive loop below the real axis. This indicates that the presence of the plant extract does not change the corrosion mechanism.

The capacitive loop at high frequency is related to the oxide film on the aluminium surface.

The inductive loop at low frequency is attributed to the slow relaxation of $O_{2(g)}$ adsorption process, oxide dissolution and aluminium dissolution reactions [15]. The capacitive behavior of the impedance indicates that the perturbation of the alloy surface by small alternating potential signals with an amplitude of 10 mV cause the dissolution process of the alloy to be controlled by the charge transfer process from the anodic sites (aluminium) to cathodic sites (Cu and Fe containing intermetallic.

The theoretical equivalent circuit shown in Figure (7) is used to analyze the impedance spectra. This circuit includes the solution resistance R_s, a series combination of resistance ® and inductance (L) in parallel with charge transfer resistance (R_{ct}) and the constant phase element (CPE), Q.

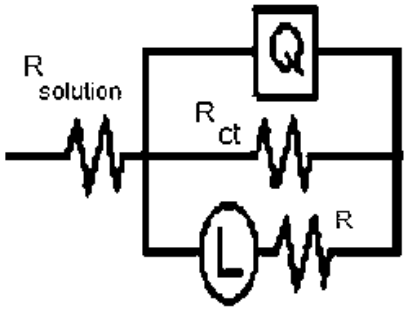

Figure 7. The theoretical equivalent circuit used to fit the experimental impedance diagrams.

In the high frequency limit, the inductive contribution to the overall impedance is insignificant. Therefore, the Nyquist plot of the impedance has a semicircle characteristic of the parallel arrangement of the double layer capacitance and a charge transfer resistance corresponding to the aluminium dissolution reaction ($Al\text{-}Al^{+}$). Contribution to the total impedance at intermediate frequencies comes mainly from the charge transfer resistance and inductive component in parallel. The inductor arises from adsorption processes of oxygen gas in an intermediate species such as $Al^{+}_{ads.}$ and $Al^{3+}_{ads.}$ This could be defined as ($L=R\tau$), where τ is the relaxation time for the adsorption process at the electrode/solution interface. The low frequency locus displays the characteristics of parallel RC circuit [16]. The Q-component used in this model to compensate for non-homogeneity in the system and is defined by two values, C and *n*. The impedance of Q is represented by

$$Z_Q = C^{-1} (i\omega)^{-n}$$

Where, C is the capacitance, $i = (-1)^{1/2}$, ω is Frequency in $rad.s^{-1}$, $\omega = 2\pi f$ and *f* is the frequency in Hz. If n = 1.0, CPE is identical to that of a capacitor and $Z_c = (i\omega C)^{-n}$ and Q correspond to a pure capacitance. For non-homogeneous system, *n* = 0.9-1.0. The value of Q is expressed in $Ohm.sec^2.cm^{-2}$ or micro-Farad (μF).

The aluminium surface is energetically heterogeneous due to the local disordering, different crystallographic forces, surface roughness, and impurities presence of various pores of different size and shapes that strongly influence the adsorption at metal/solution interface [17].

On using (Z simpwin) analysis software program, the theoretical equivalent circuit, Figure (7) fitted well with the impedance spectrum with small error and the impedance. See Tables (4-6).

Table 4. The electrochemical impedance parameters of dissolution of of 7075-T6 aluminium alloy in 0.5M NaCl at 30°C in absence and presence of different concentrations of Damsissa extract.

Extract conc. (g/L)	R1(sol.) (ohm.cm^2)	Q_{dL} (µF)	R2 (ohm.cm^2)	Inductance (Henri.cm^2)	n	Rct (ohm.cm^2)	% P
Blank	23.97	16.63	1.003×10^4	985	0.8543	4050	0
0.005	26.41	10.32	3.856×10^4	1563	0.8820	5864	30.9
0.010	24.95	9.96	4.888×10^4	2045	0.8436	6900	41.3
0.020	31.81	9.41	7.652×10^4	2986	0.916	8150	50.3
0.030	31.91	9.00	9.035×10^4	3422	0.9026	9358	56.7
0.040	32.96	8.37	1.2015×10^5	4009	0.9234	11330	64.3
0.070	23.29	13.29	8.780×10^4	2793	0.8000	8098	50.0

Table 5. The electrochemical impedance parameters of dissolution of 7075-T6 aluminium alloy in 0.5M NaCl at 30°C in absence and presence of different concentrations of Lupine extract.

Extract conc. (g/L)	R1 (ohm.cm^2)	Q_{dL} (µF)	R2 (ohm.cm^2)	Inductance (Henri.cm^2)	N	Rct (ohm.cm^2)	% P
Blank	23.97	16.62	1.059×10^4	1050	0.8539	4050	0
0.0005	18.72	15.99	1.336×10^4	1115	0.8642	4686	13.6
0.001	23.14	12.07	1.865×10^4	1588	0.9011	5250	22.9
0.003	22.53	11.91	2×10^4	1591	0.9153	5324	23.9
0.005	21.45	10.03	2.587×10^4	1814	0.9013	6263	35.3
0.030	25.47	9.87	2.996×10^4	2634	0.8906	7159	43.4
0.050	26.09	9.36	3.702×10^4	3014	0.8949	8428	51.9
0.070	30.92	9.034	3.904×10^4	3456	0.9172	8751	53.7
0.090	38.82	9.00	3.997×10^4	3560	0.8964	8975	54.9
0.150	24.56	8.22	5.301×10^4	4615	0.8874	13940	70.1
0.200	27.18	8.13	5.699×10^4	4840	0.9103	16410	75.3
0.230	22.19	7.16	6.160×10^4	6795	0.9150	24700	83.6
0.26	27.4	8.18	5.501×10^4	4708	0.9259	14803	72.6

Table 6. The electrochemical impedance parameters of dissolution of 7075-T6 aluminium alloy in 0.5M NaCl at 30°C in absence and presence of different concentrations of Halfa-Bar extract.

Plant extracts conc. (g/L)	R1 (ohm.cm^2)	Q_{dL} µF	R2 (ohm.cm^2)	Inductance (Henri.cm^2)	N	Rct (ohm.cm^2)	% P
Blank	24.98	16.06	1 x 10^4	1003	0.8542	4050	0
0.005	23.95	15.32	2.674 x 10^4	1932	0.8725	6038	32.9
0.015	22.18	15.32	2.726 x 10^4	2630	0.8558	6637	39.0
0.025	16.66	15.65	2.700 x 10^4	2600	0.9208	6630	38.9
0.040	20.23	15.10	2.770 x 10^4	2695	0.8625	6702	39.6
0.050	18.88	9.01	3.016 x 10^4	3012	0.9081	7644	47.0
0.060	22.84	8.08	4.123 x 10^4	4963	0.9153	10740	62.3
0.070	26.63	7.47	5.455 x 10^4	7999	0.9256	10886	62.8
0.090	26.94	8.15	5.000 x 10^4	7230	0.9126	10800	62.5
0.180	23.23	8.33	4.683 x 10^4	6700	0.9487	10350	60.9
0.250	26.65	8.54	4.006 x 10^4	4321	0.9240	9497	57.4

The decrease in the values of capacitance of the double layer with increasing the concentration of the plant extracts indicates the adsorption of their phytochemical constituents on aluminium surface. The relaxation time, (τ = L/R) that measures the rate at which, non-equilibrium distribution decays out towards the equilibrium distribution is found to be of the order of 10^{-4} sec. for all tested solution indicating the occurrence of adsorption of various intermediates on aluminium surface.

The inhibition efficiency of plant extracts is calculated from the following relation:

$\% P = (1/R_{cto} - 1/R_{ct})/1/R_{ct}) \times 100$

Where, $1/R_{cto}$ and $1/R_{ct}$ represent the reciprocal of charge transfer resistance of different concentrations of plants extracts respectively.

The maximum %P obtained for Damsissa extract is 64.3% at the critical concentration 0.040 g/L, for Lupine extract, 83.6% at 0.230 g/L and for Halfa-Bar extract, 62.8% at 0.070 g/L. The critical concentrations of extracts differ due to the difference in the nature of phytochemical constituents of these extracts.

3.3. Application of adsorption isotherms

The understanding of the nature of the adsorption process of the investigated extracts on aluminium surfaces is essential to our knowledge of their inhibition mechanism. The action of an

inhibitor in neutral media is assumed to be due to its adsorption at the metal/solution interface [18].

The chemical constituents of *Ambrosia maritime* L. (Damsissa) contain an important sesquiterpene lactones and flavonoids which showed molluscicidal and cytotoxic activities. The most active compounds of this plant are damsin and ambrosin. Damsin is 2, 3-dihydroambrosin. However, ambrosin belongs to a group of natural products known as pseudoguaianolides [7].

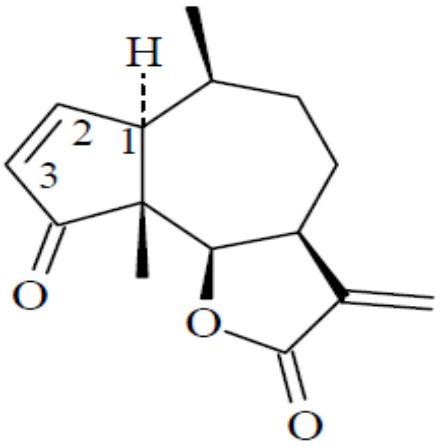

Figure 8. Chemical structural formula of ambrosin.

Lupine seeds contain up to 50% protein, 20% lipids and 5% quinolizidine alkaloids. Analysis of the alkaloid content by capillary gas chromatography clarified that, quinolizidine lupine alkaloids especially, lupanine was the most abundant and multiflorine was also present. Lupine extract contains sparteine that is dibasic quinolizidine alkaloid. It has oxytocic and diuretic properties and its sulfate salt has been used as an antiarrhythmic drug [8].

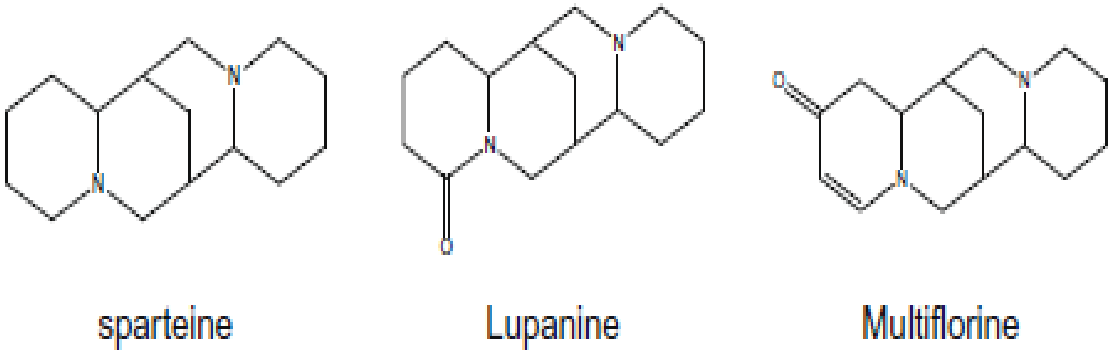

Figure 9. Chemical structural formula of sparteine, lupanine and multiflorine.

Halfa-Bar mainly used in folk medicine as it alleviate the toxic effect of carcinogens in the liver of diabetic, it acts as antispasmodic, diuretic agent and has antimicrobial activity. The main chemical compounds found in *Halfa-Bar* are six sesquiterpenes as the following sequence: proximadiol (1), 5α-hydroxy-β-eudesmol(2), 5α-hydroperoxy-β-eudesmol(3),1β-hydroxy-β-eudesmol(4),1β-hydroxy-α-eudesmol (5) and 7α, 11-dihydroxy-cadin-10(14)-ene.(6) [9].

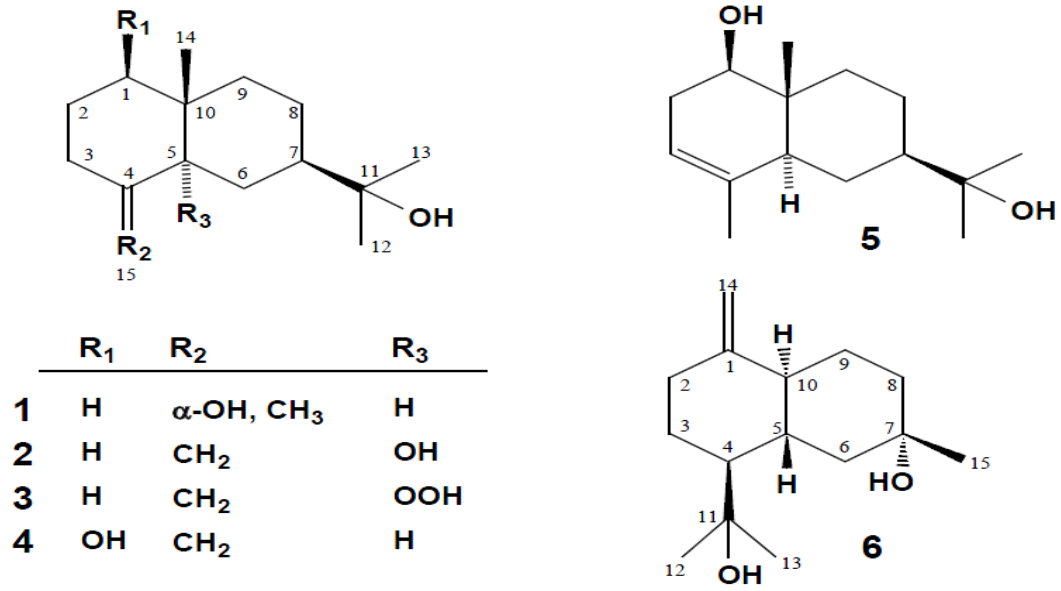

	R_1	R_2	R_3
1	H	α-OH, CH_3	H
2	H	CH_2	OH
3	H	CH_2	OOH
4	OH	CH_2	H

Figure 10. Chemical structural formula of proximadiol, 5α-hydroxy-β-eudesmol, 5α-hydroperoxy-β-eudesmol, 1β-hydroxy-β-eudesmol, and 1β-hydroxy-α-eudesmol, and 7α, 11-dihydroxy-cadin-10(14)-ene.

It is clear that, Damsisa, Lupine and Halfa-Bar extracts contain oxygen, nitrogen atoms and π-electrons bonds that may adsorb at the aluminium/solution interface. The adsorption process could take place via (i) electrostatic attraction between the charged aluminium and the charged extract molecules, (ii) dipole-type interaction between unshared electron pairs in the extract with aluminium (iii), the π-electrons bonds interaction with aluminium surface and (iv) the combination of all of these types [19].

The inhibition action is a simple substitution process, where an inhibitor molecule in an aqueous phase substitutes to *x* number of water molecules adsorbed on the metal surface [20]. The degree of fractional surface coverage (θ) of aluminium surface by an adsorbent can be calculated from the equation:

$\theta = (i_o - i)/i_o$

The inhibition efficiency of the plant, $\%P = \theta \times 100$

Where, (i_o) and (i_{corr}) are the corrosion current density (mA/cm^2) in the absence and presence of different concentrations of plant extracts.

Figure (11) illustrates the variation of the protection efficiency of the plants extracts estimated from the polarization data versus the logarithm of the concentration of Damsissa, Lupine and Halfa-bar extracts in (g/L) in 0.5M NaCl at 30°C. Each adsorption isotherm shows that there is a critical concentration that must not be exceeded in the testet solution. The adsorption isotherm for Damsissa follows the normal S-shape isotherm, Whereas the adsorption isotherm for Lupine shows two steps and that of Halfa-bar shows a slow rising part of surface coverage with increasing the concentration of the plant extract. The rising part from each isotherm is tested to the Langmuir, Flory-Huggins adsorption isotherm and the kinetic-thermodynamic model.

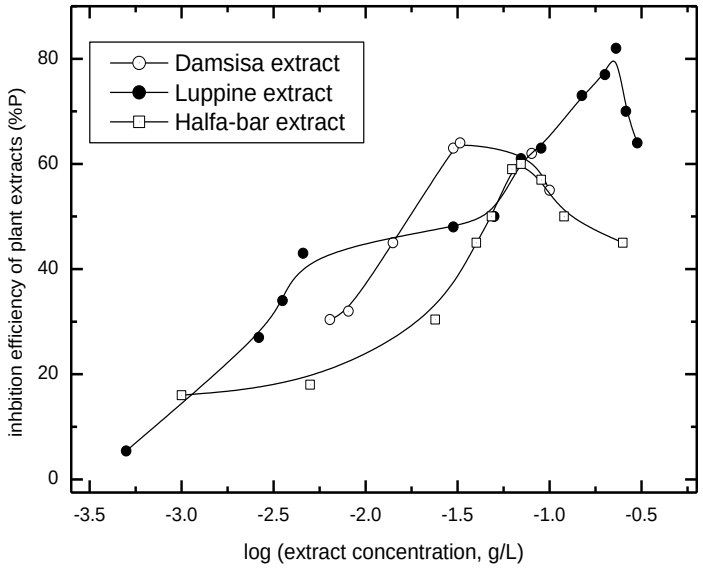

Figure 11. Adsorption isotherm of plant extracts for corrosion of 7075-T6 aluminium alloy in 0.5M NaCl at 30^{o}C.

The adsorption isotherm of Damsissa extract indicates that this extract fills only the micropores on the alloy surface and that the existence of unfilled mesopores or macropores may be probable. The adsorption isotherm of Lupine indicates filling all the pores on the alloy surface. On the other hand, the adsorption isotherm of Half-bar extract indicates that there is weak interaction between this extract and the alloy surface. The rising part of each adsorption isotherm corresponds to the binding or equilibrium constant, K of the adsorption process of the plant extract on the alloy surface. The adsorption process has first order kinetics at low concentration of the plant extract, where %P varies linearly with concentrations of the plant extract. The plateau or saturation region corresponds to the maximum rate of adsorption and it obeys zero order kinetics [21].

Since, the surface concentration of the plant extracts is related to surface coverage, θ, the Langmuir, Flory Huggins adsorption isotherms and Kinetic-Thermodynamic model were tested for the values of surface coverage θ of the three plants extracts.

- Langmuir isotherm [21].

$[\theta / (1- \theta)]=K[C]$

- Flory-Huggins isotherm [22].

$\theta /[x(1- \theta)^{x}] = K[C]$

- Kinetic - thermodynamic model is given by [23].

$\log [\theta / (1- \theta)] = \log K' + y \log C$

Where,

y: number of inhibitor molecules occupying one active site.

K: the binding constant represent the interaction of plant extract with aluminium surface

$K= K'^{(1/y)}$

This model looked to the adsorbent action from a purely mechanistic point of view and considered that the corrosion experiment carries all the features of a kinetic investigation under pseudo zero order conditions and the reaction rate = k_{obs}.

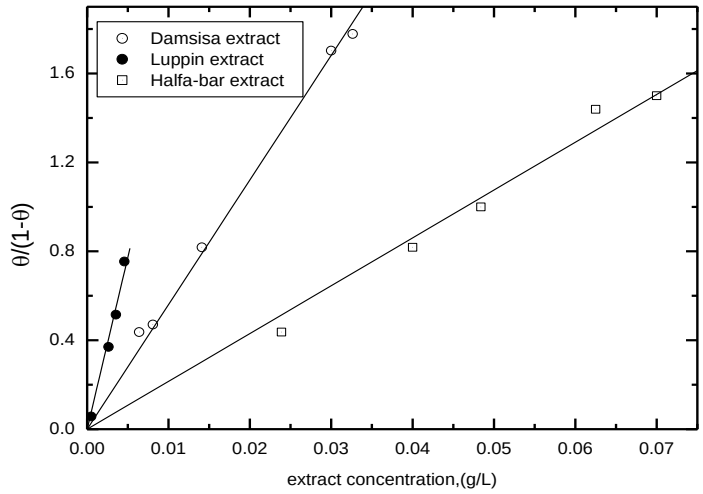

Figure 12. Linear fitting of 7075-T6 aluminium alloy dissolution in 0.5M NaCl containing different concentrations of plant extracts to Langmuir adsorption isotherm at 30^{o}C.

Figure (12) shows the application of Langmuir adsorption isotherm to the values of surface coverage θ.

Langmuir is applicable to all values of (θ) for aluminium alloy dissolution in all the inhibited solutions.

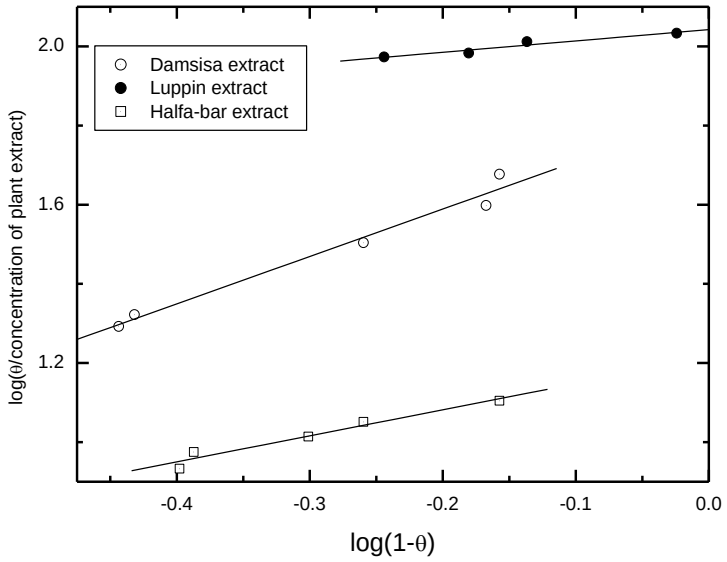

Figure 13. Linear fitting of 70-75T6 aluminium alloy dissolution in 0.5M NaCl containing different concentrations of plant extracts to Flory-Huggins adsorption isotherm at 30^{o}C.

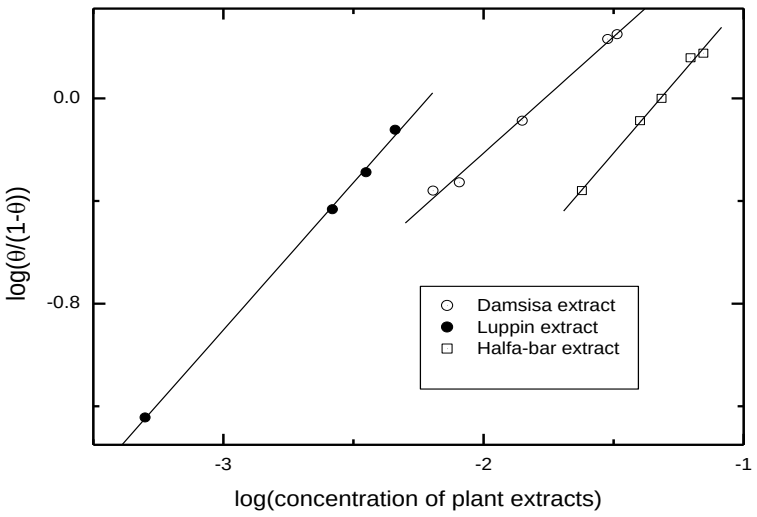

Figure 14. Linear fitting of 7075-T6 aluminium alloy dissolution in 0.5M NaCl containing different concentration of plant extracts to the kinetic-thermodynamic model at 30^{o}C.

This indicates that the surface of the alloy is uniform; all adsorption sites are equivalent for all values of fractional coverage (θ) of the alloy surface by the plants extracts. There is no lateral interaction between the adsorbed molecules regardless of the surface coverage (θ). The equilibrium adsorption coverage attained rapidly and reversible. Moreover, the free energy of adsorption, ΔG_{ads} is the same on the overall aluminium surface [24].

Figures (13, 14) represent the testing of Flory-Huggins and the kinetic-thermodynamic model to the experimental values of θ.

The good fitting of the experimental data to the kinetic-thermodynamic model indicates that the role of the plant extracts on the corrosion rate of the aluminium alloy in 0.5M NaCl has both kinetic and thermodynamic implications.

Table 7. The calculated parameters for 7075-T6 aluminium alloy dissolution in 0.5M NaCl at 30^{o}C, to the linear fitting to Langmuir, Flory-Huggins adsorption isotherms and the kinetic-thermodynamic model.

Extract	Calculated parameters				
	Langmuir	Kinetic-thermodynamic		Flory-Huggins	
	K	K	1/y	K	X
Damsissa	56	58.17	1.1	56.25	1.19
Lupine	155	164	0.87	384	0.287
Halfa-Bar	21.5	20.9	0.85	24.77	0.66

The values of (1/y) represent the number of the active sites of the surface occupied by one inhibitor molecule and 1/y ≈ 1.0 indicates that each inhibitor molecule occupies one active site. X is the size ratio is unexpected for Lupine extract; i.e. the kinetic model is more preferable for describing the experimental data.

Since the efficiency of a given inhibitor was essentially a function of the magnitude of its binding constant K, large values of K indicate better and stronger interaction, whereas small values of K mean that the interaction between the inhibitor molecules and the metal is weaker [25,26,27].

According to the numerical values of K obtained from Flory-Huggins adsorption isotherm or the kinetic-thermodynamic model, the inhibition efficiency of the plant extracts follows the order:

Lupine > *Damsissa* > *Halfa-Bar*.

Lupine extract has the highest inhibition efficiency for the corrosion of 7075-T6 aluminium alloy in 0.5M NaCl at 30^{o}C, while Halfa-Bar has the least inhibition efficiency.

3.4. The adsorption mechanism

The expected mode of adsorption process on the aluminium surface in 0.5 M NaCl is the adsorption of chloride ion on the positively charged aluminium surface rather than the protonated forms of phytochemicals of plant extracts. The inhibition of aluminium corrosion by the plants was initiated by physical adsorption, which was strengthened by chemisorption of phytochemicals of plant extracts on the aluminium surface. Chemisorption is attributed to an aluminium surface which has vacant P valence orbitals, such that it is likely to function as a Lewis acid (electron-pair acceptor) from the heteroatoms (O, N) or OH group in the phytochemicals of the plant extracts. This type of interaction results in coordinate bond formation to the aluminium surface.

The chemical structure of Lupine extract contains more heteroatoms (nitrogen atoms) than Damsissa and Halfa-bar extracts. Due to the electron negativity of: N > O > OH, lupine extract offers the strongest chemisorptions, while Halfa-bar extract offers the least extent of chemisorption [28].

4. CONCLUSIONS

- For dissolution of 7075-T6 aluminium alloy in 0.5M NaCl at 30^{o}C, the aqueous extracts of Damsisa, Lupine and Halfa-bar plants act as cathodic type inhibitors which retard the partial cathodic reaction of the corrosion process.

- The inhibition efficiency of these extracts is mainly due to their adsorption on the alloy surface.

- Lupine extract has the highest inhibition efficiency while Halfa-bar extract has the lowest inhibition efficiency for dissolution of the alloy in 0.5M NaCl. This trend may be related to the chemical structure of their phytochemical constituents.

References

1. K.F. Blurton, A.F. Sammells, *J. Power Sources* 4 (1979) 263.
2. Julie-Anne Hill, Tracey Markley, Maria Forsyth, Patrick C. Howlett and Bruce R. W. Hinton, *Journal of alloys and compounds*, 509 (2011) 1683.
3. R. E. Smallman and R. J. Bishop, Modern Physical Metallurgy and Materials Engineering, Elsevier Butterworth-Heinemann, 1999.
4. Q. Meng, G.S. Frenkel, *Journal of the Electrochemical Society* 151 (2004).
5. M. Schumacher, Seawater Corrosion Handbook, William Andrew Publishing/Noyes, 1979.
6. M. Dabala, E. Ramous, M. Magrini, *Materials and Corrosion* 55 (2004) 381–386.
7. N. M. Abdel-Hamid, V.E. Tarabanko, Radioprotective Effect of an Egyptian wild Herb *Ambrosia Maritimal*., (2004) 53.
8. A. M. Abdel-Gaber, B.A. Abd-El-Nabey, M. Saadawy, *Corros. Sci*., 51 (2009) 1038.
9. L. L. Sherier , R. A. Jarman and G. T.Burstein, Corrosion Contol, Oxford, U. K. Butter Worth Heinenmann (1994).
10. R. Roslizaa,b, W.B. Wan Nik, *Current Applied Physics* 10 (2010) 221.
11. M. Darzic, 11th Power Sources mp, Brighton, England (1978).
12. R. Despic and P.D. Millanpvie, Trav.St.Sciences Techniques, *Academic Serbia Art*, 12 (1) (1979) 1.
13. O. R. Brown, J. S. Whitley, *Electrochimica Acta*, 32 (4) (1987) 545.
14. L. M. Doche, J. J. Rameau, R. Durand, F. Novel, Cattin, *Corros. Sci.*, 41 (1999) 805.
15. H. J. W. Lendernik, M. V. D. Linden and J. H.W. Dewit, *Electrochimica Acta*, 38 (14) (1993) 1489.
16. M. Lebrini, F. Robert, A. Lecante, C. Roos, *Corrosion Science* 53 (2011) 687.
17. W. Rudzinski, O. H. Everett, London (1991).
18. K. Aramaki, Y. Node, and H. Nishihara, *J. Electrochem. Soc.*, 137 (1990) 1354.
19. D. Schweinsberg, G. George, A. Nanayakkawa, and D. Steinert, *Corros. Sci*., 28 (1988) 33.
20. B. Ateya, B. El-Anadouli, and F. El-Nizamy, *Corros. Sci*., 24 (1984) 509.
21. I. Langmuir, *J. Am. Chem. Soc*., 38 (1916) 2221.
22. P. J. Florry, *J. Chem. Phys*. 10 (1942) 51.
23. A. A. El-Awady, B. A. Abd-El-Nabey and S.G. Aziz, , *J. Electrochem. Soc.*, 19 (1992)2149.
24. S. J. Gregg, K.S. W. Sing, (Adsorption, Surface aerea and porosity), 2nd edition, Academic Press, INC (London) (1982).
25. N. Khalil, F. Mahgoub, B.A. Abd-El-Nabey and A. Abdel-Aziz, *CEST*, 38 (2003) 205.
26. B. A. Abd-El-Nabey, E. Khamis, M. Sh. Ramadan, and A. El-Gindy, *Corrosion*, 52 (1996) 671.
27. Pierre R. Roberge, Corrosion Engineering: Principles and Practice, McGraw-Hill, (2008).
28. F. Bentiss, M. Traisnell, and M. Lagrenee, *J. Appl. Electrochem*., 31 (2001) 41.